

## Coherence Scale of the Intergalactic Medium from the Gravitational Lens System CSWA 38

MADISYN BROOKS,<sup>1</sup> TUCKER JONES,<sup>2</sup> AND KEERTHI VASAN G.C.<sup>2</sup>

<sup>1</sup>*Department of Physics, University of Central Florida, 4000 Central Florida Blvd, Orlando 32816, FL, USA*

<sup>2</sup>*Department of Physics and Astronomy, University of California Davis, 1 Shields Avenue, Davis, CA 95616, USA*

### ABSTRACT

The diffuse gas between galaxies, known as the intergalactic medium (IGM), is predominantly studied through Lyman- $\alpha$  absorption lines in the spectra of bright background sources. The IGM is expected to be spatially uniform on scales  $\lesssim 100$  kpc due to pressure smoothing. The smoothing scale is sensitive to the thermal history of the IGM and is influenced by the timing of cosmological events, like reionization. Measurements of the pressure smoothing scale of the IGM can therefore provide insight into the sources responsible for reionization. We describe the methodology used to investigate the coherence scale of the intergalactic medium from the CSWA 38 lens system, a spatially resolved system, and use this scale to help constrain the time of reionization. The use of CSWA 38 for this study allows for Lyman- $\alpha$  tomography over the extent of the lensed arcs. We are able to probe the IGM at redshifts  $z \approx 2.9$  on smaller spatial scales than previous analyses of quasar-pair systems. Our results present a smooth IGM on small cosmic scales; we find no significant changes in the width or line center of 5 different Ly $\alpha$  absorbers on scales of  $\lesssim 70$  comoving kiloparsecs. We additionally find consistent hydrogen column densities of  $N_{\text{HI}} \sim 10^{14} \text{ cm}^{-2}$ . Our results are consistent with expectations from hydrodynamical cosmological simulations with standard model parameters, which confirms that the IGM is indeed smooth on spatial scales  $\lesssim 100$  kpc.

### 1. INTRODUCTION

The bulk of the baryonic matter in the universe resides in the diffuse gas in the spaces between galaxies, known as the intergalactic medium (IGM). Understanding the evolution of the IGM is a useful tool for constraining important cosmological parameters, like the time and cause of reionization, the cosmic mean density, and the nature of cold dark matter (e.g., Hui & Gnedin 1997; Abel & Haehnelt 1999; Hui & Haiman 2003; Weinberg et al. 2003; McQuinn et al. 2009; Rorai et al. 2017). The IGM is primarily studied through Ly $\alpha$  absorption lines seen in the spectrum of background quasars. This so-called Ly $\alpha$  forest is a valuable tool to understand the thermal evolution of the IGM at redshifts  $z \sim 2-5$  and thus to help constrain the time of reionization. In particular, the IGM pressure smoothing scale contains a record of the thermal history of the Universe (Rorai et al. 2013). At large scales, the IGM follows the structure determined by density fluctuations, which are influenced by the underlying dark matter distribution. At small scales, the baryonic matter in the IGM experiences pressure forces which results in characteristic smoothing relative to the otherwise clumpy dark matter distribution (Gnedin & Hui 1998; Kulkarni et al. 2015). The pressure smoothing scale

is sensitive to the temperature of the IGM and the temperature of the IGM in the past. The smoothing scale reflects reionization heating timescales over the Universe's history, thus we can use the IGM to investigate the timing and cause of reionization heating events.

The smoothing scale is sensitive to reionization history, therefore different models of reionization will change the spatial scales in which we begin to see pressure smoothing affect the structure of the IGM. Late reionization heating models predict a smaller pressure smoothing scale, while increased heating models predict a larger smoothing scale. We do not expect to see any structure in the IGM on scales smaller than 70 comoving kiloparsecs, as predicted by the hydrodynamical simulations from Rorai et al. (2017). This follows from a reionization model that is based on standard model cosmology (Haardt & Madau 2012). Current work does not probe below this separation and does not confirm that the IGM is smooth as predicted by our current cosmological models.

Quasar systems have been studied for decades and have provided a wealth of information about the neutral hydrogen fraction of the universe and the column density distribution of Ly $\alpha$  absorbers, but since they give us a pencil-beam view through the IGM, they only

provide line-of-sight information. However, even line-of-sight structure is complicated to interpret on small scales due to peculiar velocities. Some promising work on transverse spatial structure has been done using multiply imaged lensed quasars and close pairs (e.g., Smette et al. 1995; Coppolani et al. 2006; D’Odorico et al. 2006; Maitra et al. 2019; Fan et al. 2022), but such alignments are rare and still provide limited lines of sight. Extended background sources – namely bright gravitationally lensed arcs – have recently been used to map the spatial structure of CGM around  $z \lesssim 1$  galaxies (Lopez et al. 2018; Mortensen et al. 2021) and of damped Ly $\alpha$  (DLA) systems associated with dwarf galaxies (Bordoloi et al. 2022). This technique of lensed arc tomography has the advantage of allowing us to probe smaller spatial scales than with quasar-pair systems, and offers continuous spatial sampling.

The goal of this paper is to investigate the coherence length scale of the IGM due to pressure and temperature smoothing effects, via direct measurements on small transverse spatial scales ( $\lesssim 100$  comoving kiloparsecs). Specifically we aim to resolve regions below the predicted smoothing scale of  $\sim 70$  comoving kpc at  $z \sim 2.5 - 3$  (e.g., Rorai et al. 2017). In this work, we probe the spatial distribution of Ly $\alpha$  absorbers in the IGM based on spatially resolved spectroscopy of CSWA 38, a gravitational lens system cataloged in the Cambridge and Sloan Survey of Wide ARcs in the sky. This system houses two extended, bright arcs, which are used to perform a tomographical study of the Ly $\alpha$  forest. We analyze the Ly $\alpha$  absorption line profiles across the extent of the system and calculate neutral hydrogen column densities.

The structure of this paper is as follows. In Section 2 we give a brief overview of the spectroscopic observations and data reduction. Section 3 describes the lens model used to calculate spatial separations in each absorber plane, and the methods for fitting absorption lines and measuring hydrogen column density. We present our main results in Section 4 and our discussion and conclusions follow in Section 5. In this work, we adopt a concordance cosmology with  $H_0 = 70 \text{ km s}^{-1} \text{ Mpc}^{-1}$ ,  $\Omega_m = 0.26$ , and  $\Omega_\Lambda = 0.74$ . In this cosmology, one arcsecond corresponds to 7.912 kpc at  $z = 2.9$ .

## 2. SPECTROSCOPIC DATA

CSWA 38 was observed with the Keck Cosmic Web Imager (KCWI; Morrissey et al. 2018) on four nights during three separate observing runs for a total of 5.8 hours integration time. Full information on the observations, instrument configuration, and data processing is described in Mortensen et al. (2021). In

brief, we used the medium slicer (with  $0''.68 \times 0''.29$  spatial sampling, the notation  $0''.68$  denotes a fraction of an arcsecond) and BL grating configured for wavelength coverage from 4000–6300 Å. The spectral resolution is 2.4 Å full width at half maximum or  $R \approx 1800$  at the wavelengths relevant for this work. Two orthogonal position angles were used to better sample the point spread function. Data were reduced using the KCWI data reduction pipeline (KDERP) version 1.0.2. Individual reduced exposures were aligned and combined with a weighted mean. The final resulting data cube after combing all reduced exposures has  $0''.3$  spatial pixels, which adequately samples both the native pixel size and the seeing ( $\sim 1''$ ). The subsequent analysis in this paper uses this final data cube. A white-light image from this cube is shown in Figure 1.

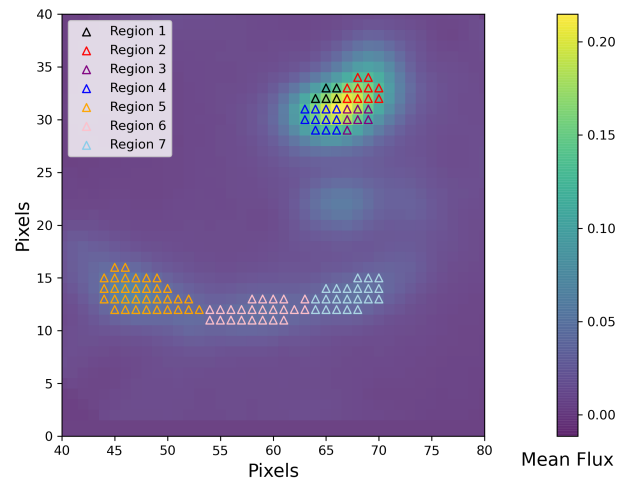


**Figure 1.** Map of CSWA 38 with individual spaxels colored for different regions. Arc 1 (top) and Arc 2 (bottom) are separated into 4 and 3 regions, respectively, with their respective regions having similar areas. The background image is a collapsed KCWI white light data cube. The pixel size is  $0''.3$ .

## 3. METHODOLOGY

The CSWA 38 system includes two bright and extended blue arcs at a redshift of  $z = 2.92$ , which together span  $\sim 10$  arcseconds across the sky. This configuration is excellent for studying the transverse spatial structure of the IGM through Ly $\alpha$  absorption lines. The KCWI data used in our analysis probes the Ly $\alpha$  forest at redshifts  $z = 2.31 - 2.92$ , and our chosen Lyman alpha absorbers cover the redshift range  $z = 2.51 - 2.77$ .

The two bright gravitationally lensed arcs in the CWSA 38 system were divided into 7 spatial bins, shown in Figure 1. This was done to allow for spatial sampling of smaller distances within the individual arcs, and for larger distances between the two arcs. These spatial bins were chosen to achieve good signal/noise within each binned region, sufficient to obtain good fits to Ly $\alpha$  forest absorption lines. Arc 1 and arc 2 were first separated into regions of equal areas and then the spaxels were individually checked for Ly $\alpha$  line detection. For arc 1, a spaxel was included in the region if the mean flux was  $\geq 0.1$ . Since arc 2 is significantly fainter than arc 1, the spaxel acceptance criteria we adopted was a sum of the total flux  $\geq 25$ . The spaxels were binned together into the selected regions, as opposed to fitting each individual spaxel, to increase our S/N. We then chose a spaxel coordinate to represent the center of each region and found the distance between the region centers in comoving kiloparsecs, determined at the redshift of each absorber using the gravitational lens model (Section 3.2). The center of the binned regions are defined by their geographical center.

For this analysis, we focus on transverse spatial variation measurements for a subset of 5 Ly $\alpha$  absorbers which are well detected and cleanly resolved in the spectra. While this is a small fraction of the observed Ly $\alpha$  forest, using unblended features allows us to minimize systematic errors in the line profiles and H I column density. To quantify the transverse spatial variation, we fit Gaussian profiles to 5 Ly $\alpha$  absorbers at the following redshifts:  $z = 2.513, 2.549, 2.712, 2.720, \text{ and } 2.765$  for each of the 7 spatial regions. The individual absorbers used in this analysis are shown in Figure 2. We then calculated the difference in both the line width (FWHM) and line centroid for each pair of regions, and repeated this process for each absorber. This procedure provides measurements of the change in Ly $\alpha$  absorber line shape across varying spatial separations. A spatial map of the centroid values of the  $z = 2.721$  absorber is shown as an example in Figure 3.

### 3.1. Voigt Profile Fitting

While the Gaussian fitting described above provides straightforward assessment of the profile shape with minimal free parameters, a Voigt profile is physically better motivated and allows us to extract information about the neutral hydrogen content. The Voigt profile describes the intrinsic shape of the absorption line profile because it combines effects from Doppler broadening, the thermal motion, and pressure broadening effects (Davé et al. 1997). Here we fit a Voigt profile to each of our Ly $\alpha$  absorber lines across the different CWSA 38

regions (e.g., Figure 4). The Voigt profile fit allows us to calculate the optical depth  $\tau$  which is in turn related to the neutral hydrogen column density. The optical depth is calculated by integrating over the Voigt profile fit. The corresponding column density for each Ly $\alpha$  absorber is determined from the following formula:

$$\tau = f\lambda \frac{\pi e^2}{m_e c} \times N = \frac{f\lambda}{3.768 \times 10^{14}} \times N \quad (1)$$

where  $f$  is the ion oscillator strength,  $\lambda$  is the rest-frame wavelength of the transition in  $\text{\AA}$ , and  $N$  is the column density expressed in  $\text{cm}^{-2}(\text{km s}^{-1})^{-1}$ . Here we adopt the value  $f = 4.164 \times 10^{-1}$  for Ly $\alpha$ .

### 3.2. Gravitational Lens Model and Reconstruction

A gravitational lens model is required to determine the true spatial separations of the different arc regions shown in Figure 1, at the redshift of each absorption system considered in our analysis. The lens model used for this work is fully described in Section 3 of Mortensen et al. (2021). This model includes the complex mass distribution of the  $z = 0.43$  galaxy cluster, as well as lensing by the nearby  $z = 0.77$  galaxy located between the arc 1 and arc 2 images. Figure 3 shows an example of the arc regions reconstructed in the  $z = 2.721$  absorber source plane (cf. their image plane locations shown in Figure 1). The source plane separations of the various regions span  $\simeq 5\text{--}70$  comoving kpc at this redshift. The absorbers studied in this work have slightly different source plane locations, depending on the redshift, but are generally similar to that shown in Figure 1. These reconstructions allow us to calculate transverse distances between each pair of regions in the appropriate source plane.

## 4. RESULTS

Over the five Ly $\alpha$  absorbers that we analyzed, we find no significant change, given the measurement uncertainties, in the Gaussian FWHM line width or centroid across the spatial separations spanned by the two arcs. For our  $z = 2.721$  absorber, the FWHM measurements are consistent within  $0.992 \text{ \AA}$ , which falls within the  $1\sigma$  uncertainty of  $1.23 \text{ \AA}$ . The  $\sigma_{\text{rms}}$  of our FWHM differences is  $= 0.477 \text{ \AA}$ . Since the measurements are consistent with our  $1\sigma$  uncertainty, this indicates that there is no evidence for variation across separations from 5 - 70 comoving kiloparsecs. A similar pattern is repeated for the centroid differences of the  $z = 2.721$  Ly $\alpha$  absorber. We find the centroids of our 7 regions to be consistent within  $0.486 \text{ \AA}$ , which is less than our  $1\sigma$  of  $0.622 \text{ \AA}$ . Figure 5 shows an example of the width difference and centroid difference

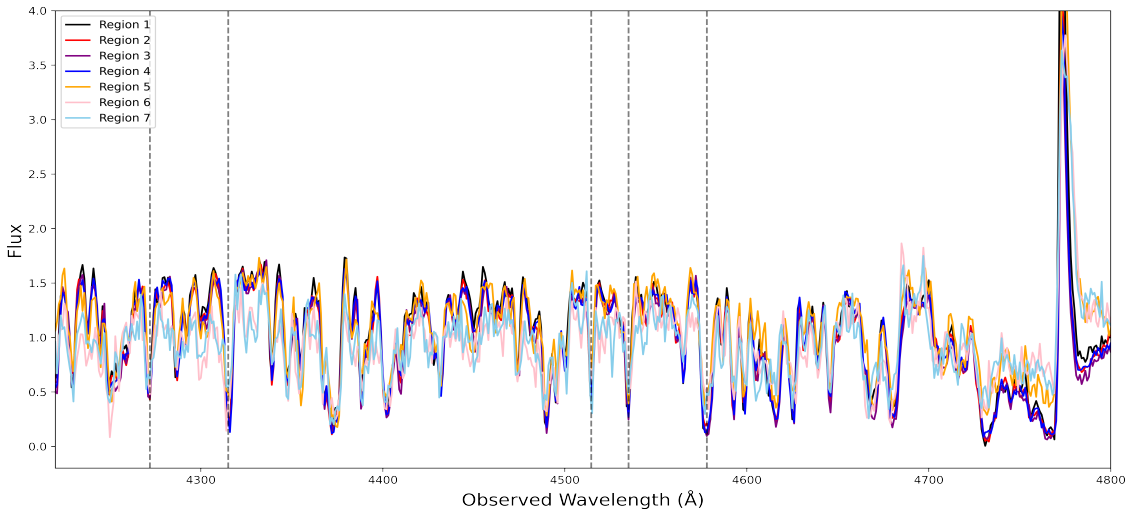


**Figure 2.** Spectra of the Ly $\alpha$  forest region for the 7 spatial regions used in this analysis. The spectra are normalized by dividing each individual spectra by its mean. The spectra clearly show similar structure in the Ly $\alpha$  IGM absorption across all seven regions. In this work we focus on the transverse spatial structure of 5 unblended Ly $\alpha$  absorbers, shown by the dashed lines.

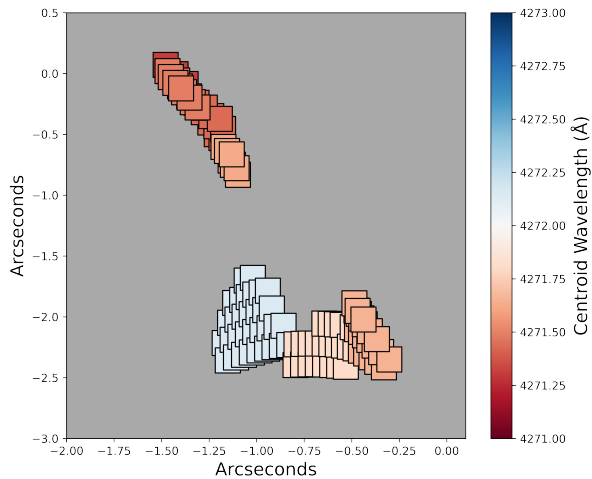


**Figure 3.** Spatial map of the  $z = 2.721$  absorber wavelength centroid values, calculated from Gaussian fits to the spectrum of each region. This map is in the source plane of the absorber which is reconstructed using the gravitational lens model. The centroids are consistent within  $0.49 \text{ \AA}$ , which is consistent with our  $1\sigma$  of  $0.62 \text{ \AA}$ . Therefore, we find no evidence for structure in the absorber redshift across the measured region.

for the  $z = 2.721$  absorption line. We find similar trends for the other absorbers included in our analysis. At these spatial scales, of less than 70 comoving kiloparsecs, we do not expect to see structure in the intergalactic

medium due to pressure smoothing effects (Rorai et al. 2013; McQuinn 2016). These results are consistent with the hydrodynamical simulations discussed in Rorai et al. (2017). We find a smooth, coherent IGM at spatial scales  $\lesssim 100 \text{ kpc}$ , which agrees with the  $\Lambda\text{CDM}$  standard model with reionization starting at  $z = 15$  (Haardt & Madau 2012; Rorai et al. 2017).

We find neutral hydrogen column densities on the scales of  $\sim 10^{14} \text{ cm}^{-2}$ , which is expected for low density Ly $\alpha$  systems (Hu et al. 1995). We find that the hydrogen column densities change by  $\sim 11\%$  over 60 comoving kpc. The  $\sim 11\%$  variation we find in the column density is consistent with our estimated  $\sim 13\%$  uncertainty, indicating no evidence for variation in hydrogen column density across 60 comoving kiloparsecs. Figure 6 shows a spatial map of the neutral hydrogen column density for the  $z = 2.721$  absorption line. We were unable to fit the Voigt profile to absorption lines in our identified region 6 due to low S/N and we do not include this region in our analysis. These trends in the hydrogen column densities further confirms our conclusion of a smooth IGM on the spatial scales we are probing using our gravitationally lensed system. Using the hydrogen column density distribution as a means of investigating the coherence of the IGM, allows us to reach a more robust conclusion that is not dependent only on the absorption line shape.

## 5. SUMMARY AND CONCLUSIONS

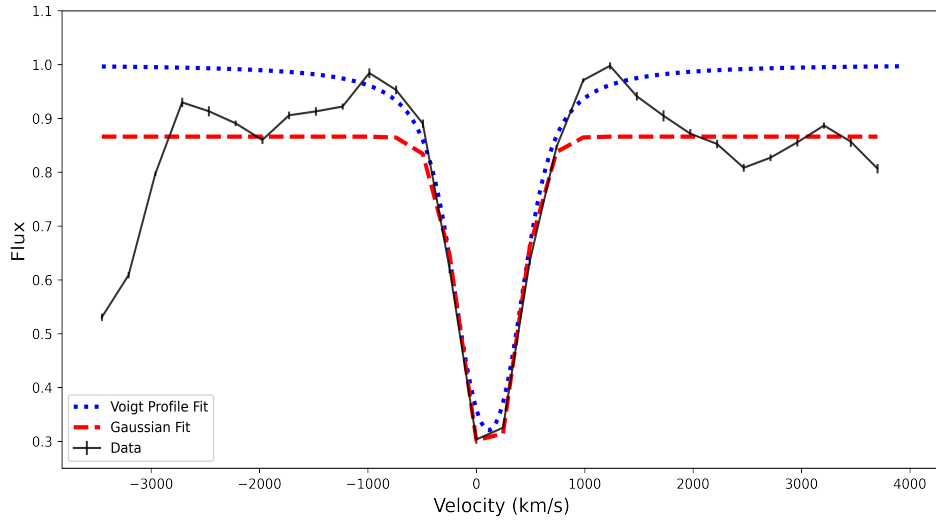


**Figure 4.** Voigt profile fit (blue) and Gaussian fit (red) of the  $z = 2.721$  Ly $\alpha$  absorber from region 1 of our binned spatial regions. The Voigt profile is used to calculate the neutral hydrogen column densities of our Ly $\alpha$  absorbers while the Gaussian fit is used to study how the absorption line profile changes over the lens system.

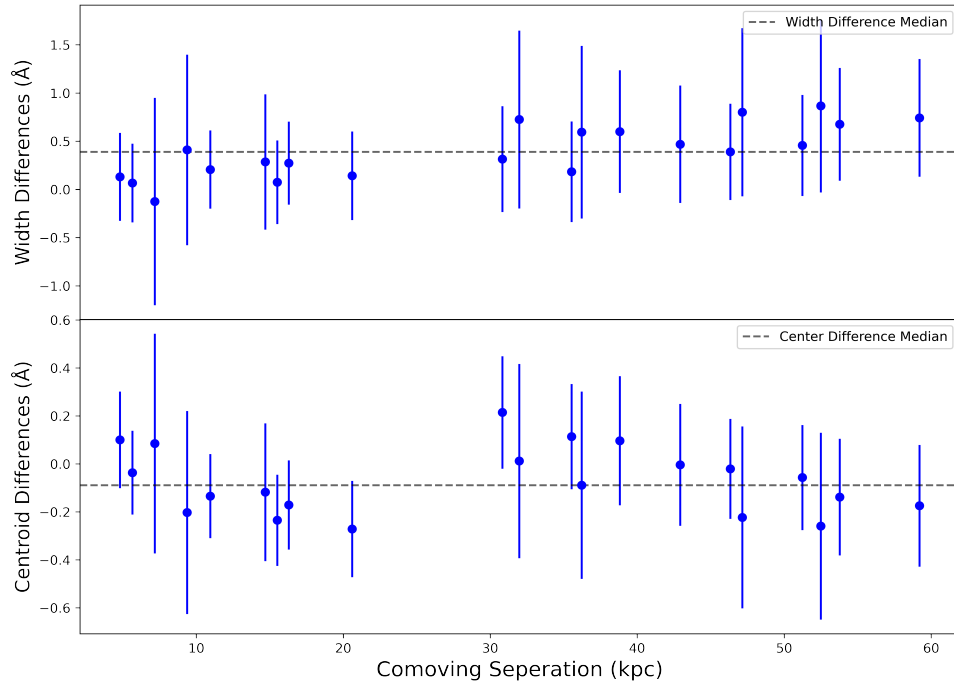


**Figure 5.** Difference between the Gaussian FWHM line widths (top) and Gaussian centroid values (bottom) between the centers of the CSWA38 regions for the  $z = 2.721$  absorber. The medians of the width difference measurements and centroid difference measurements are shown with the dashed black lines.

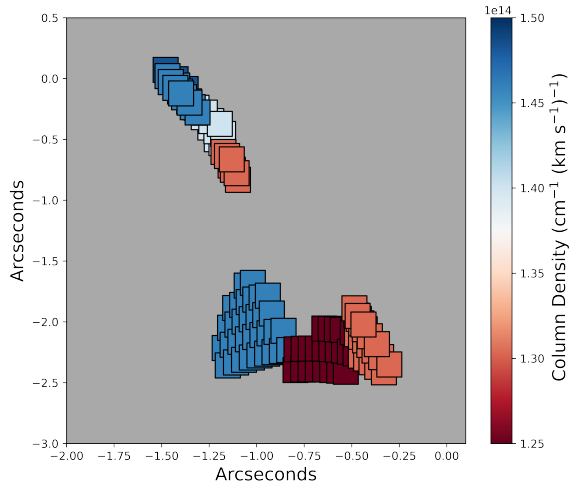


**Figure 6.** Spatial map of calculated neutral hydrogen column density in the plane of the  $z = 2.721$  Ly $\alpha$  absorption line. CSWA 38 region 6 (dark maroon) was not well fitted with the Voigt profile. We find a variation in the neutral hydrogen column density across the lens system of  $\sim 11\%$ , which is consistent with no variation within our estimated errors.

We have investigated the coherence of the intergalactic medium through the use of Ly $\alpha$  absorption lines in the redshift range of  $z = 2.513$ – $2.765$ . Our analysis takes advantage of highly magnified and extended arcs in the gravitational lens system CSWA 38, which allows us to probe contiguous spatial scales that were previously unreachable using quasar-pair systems. Our main results are summarized as follows:

1. For our  $z = 2.721$  Ly $\alpha$  absorber, we find variation in Gaussian FWHMs over the 7 identified regions of  $0.992 \text{ \AA}$ , which is consistent within our  $1\sigma$  uncertainty of  $1.23 \text{ \AA}$ . This indicates no change in the line FWHM across 60 comoving kiloparsecs.
2. For our  $z = 2.721$  Ly $\alpha$  absorber, we find variation in Gaussian centroids of the 7 identified regions of  $0.486 \text{ \AA}$ , which is consistent within our  $1\sigma$  uncertainty of  $0.622 \text{ \AA}$ . This indicates no change in the line centroids across 60 comoving kiloparsecs.
3. We find that neutral hydrogen column densities change on average of  $11\%$  over  $\sim 60$  comoving

kiloparsecs. This is consistent with our estimated  $\sim 13\%$  uncertainty. There is no evidence for variation in the neutral hydrogen column densities over 60 comoving kiloparsecs, the separation spanned by our gravitational lens system.

Here, we probe the diffuse IGM, which is not affected by the physical process, such as galactic winds, supernovae explosions, and stellar feedback, associated with galaxy formation and evolution (Desjacques et al. 2006; Kollmeier et al. 2006). The study of DLA’s conducted by Bordoloi et al. (2022) probes a system on the outskirts of a galaxy, which results in changes to the Ly $\alpha$  forest over small spatial scales. Bordoloi et al. (2022) finds variation in hydrogen column densities by more than an order of magnitude over 2-3 kiloparsec scales. These significant small-scale variations in the hydrogen column density can be attributed to the nearby galaxy. The lack of variation seen in our Ly $\alpha$  forest and hydrogen column densities confirms that we are tracing the diffuse gas of the IGM.

This work represents the first tomographic study of the intergalactic medium on spatial scales  $\leq 100$  kpc. Such analysis is important to further our understanding of the time and cause of reionization events, which influence the coherence scale of the IGM. Our results are consistent with what is predicted of standard model cosmology hydrodynamical simulations (Rorai et al. 2017). This confirms the current cosmological standard model and works to create a more robust understanding of the epoch of reionization.

#### ACKNOWLEDGEMENTS

This work is based on data obtained at the W. M. Keck Observatory, which is operated as a scientific partnership among the California Institute of Technology, the University of California, and the National Aeronautics and Space Administration. The Observatory was made possible by the generous financial support of the W. M. Keck Foundation. We wish to acknowledge the very significant cultural role and reverence that the summit of Maunakea has within the indigenous Hawaiian community. This material is based on work supported by the National Science Foundation (NSF) under grants PHY-2150515 and AST-2108515.

#### REFERENCES

Abel, T., & Haehnelt, M. G. 1999, ApJL, 520, L13,  
doi: 10.1086/312136

Bordoloi, R., O’Meara, J. M., Sharon, K., et al. 2022,  
Nature, 606, 59, doi: 10.1038/s41586-022-04616-1

- Coppolani, F., Petitjean, P., Stoehr, F., et al. 2006, MNRAS, 370, 1804, doi: [10.1111/j.1365-2966.2006.10601.x](https://doi.org/10.1111/j.1365-2966.2006.10601.x)
- Davé, R., Hernquist, L., Weinberg, D. H., & Katz, N. 1997, ApJ, 477, 21, doi: [10.1086/303712](https://doi.org/10.1086/303712)
- Desjacques, V., Haehnelt, M. G., & Nusser, A. 2006, MNRAS, 367, L74, doi: [10.1111/j.1745-3933.2006.00143.x](https://doi.org/10.1111/j.1745-3933.2006.00143.x)
- D’Odorico, V., Viel, M., Saitta, F., et al. 2006, MNRAS, 372, 1333, doi: [10.1111/j.1365-2966.2006.10941.x](https://doi.org/10.1111/j.1365-2966.2006.10941.x)
- Fan, X., Banados, E., & Simcoe, R. A. 2022, arXiv e-prints, arXiv:2212.06907. <https://arxiv.org/abs/2212.06907>
- Gnedin, N. Y., & Hui, L. 1998, MNRAS, 296, 44, doi: [10.1046/j.1365-8711.1998.01249.x](https://doi.org/10.1046/j.1365-8711.1998.01249.x)
- Haardt, F., & Madau, P. 2012, ApJ, 746, 125, doi: [10.1088/0004-637X/746/2/125](https://doi.org/10.1088/0004-637X/746/2/125)
- Hu, E. M., Kim, T.-S., Cowie, L. L., Songaila, A., & Rauch, M. 1995, AJ, 110, 1526, doi: [10.1086/117625](https://doi.org/10.1086/117625)
- Hui, L., & Gnedin, N. Y. 1997, MNRAS, 292, 27, doi: [10.1093/mnras/292.1.27](https://doi.org/10.1093/mnras/292.1.27)
- Hui, L., & Haiman, Z. 2003, ApJ, 596, 9, doi: [10.1086/377229](https://doi.org/10.1086/377229)
- Kollmeier, J. A., Miralda-Escudé, J., Cen, R., & Ostriker, J. P. 2006, ApJ, 638, 52, doi: [10.1086/498104](https://doi.org/10.1086/498104)
- Kulkarni, G., Hennawi, J. F., Oñorbe, J., Rorai, A., & Springel, V. 2015, ApJ, 812, 30, doi: [10.1088/0004-637X/812/1/30](https://doi.org/10.1088/0004-637X/812/1/30)
- Lopez, S., Tejos, N., Ledoux, C., et al. 2018, Nature, 554, 493, doi: [10.1038/nature25436](https://doi.org/10.1038/nature25436)
- Maitra, S., Srianand, R., Petitjean, P., et al. 2019, MNRAS, 490, 3633, doi: [10.1093/mnras/stz2828](https://doi.org/10.1093/mnras/stz2828)
- McQuinn, M. 2016, ARA&A, 54, 313, doi: [10.1146/annurev-astro-082214-122355](https://doi.org/10.1146/annurev-astro-082214-122355)
- McQuinn, M., Lidz, A., Zaldarriaga, M., et al. 2009, ApJ, 694, 842, doi: [10.1088/0004-637X/694/2/842](https://doi.org/10.1088/0004-637X/694/2/842)
- Morrissey, P., Matuszewski, M., Martin, D. C., et al. 2018, ApJ, 864, 93, doi: [10.3847/1538-4357/aad597](https://doi.org/10.3847/1538-4357/aad597)
- Mortensen, K., Keerthi Vasam, G. C., Jones, T., et al. 2021, ApJ, 914, 92, doi: [10.3847/1538-4357/abfa11](https://doi.org/10.3847/1538-4357/abfa11)
- Rorai, A., Hennawi, J. F., & White, M. 2013, ApJ, 775, 81, doi: [10.1088/0004-637X/775/2/81](https://doi.org/10.1088/0004-637X/775/2/81)
- Rorai, A., Hennawi, J. F., Oñorbe, J., et al. 2017, Science, 356, 418, doi: [10.1126/science.aaf9346](https://doi.org/10.1126/science.aaf9346)
- Smette, A., Robertson, J. G., Shaver, P. A., et al. 1995, A&AS, 113, 199
- Weinberg, D. H., Davé, R., Katz, N., & Kollmeier, J. A. 2003, in American Institute of Physics Conference Series, Vol. 666, The Emergence of Cosmic Structure, ed. S. H. Holt & C. S. Reynolds, 157–169, doi: [10.1063/1.1581786](https://doi.org/10.1063/1.1581786)